

Comparative Study on the Binding Affinity of Methimazole and Propylthiouracil to Thyroid Peroxidase as an Anti-Thyroid Drug: An *In-silico* Approach

Sushmita Pradhan, Himakshi Sarma, Barsha Bharadwaz and Venkata Satish Kumar Mattaparthi*

Molecular Modelling and Simulation Laboratory, Department of Molecular Biology and Biotechnology, Tezpur University, Tezpur-784 028, Assam, India

*Corresponding author: Venkata Satish Kumar Mattaparthi, Molecular Modelling and Simulation Laboratory, Department of Molecular Biology and Biotechnology, Tezpur University, Tezpur-784 028, Assam, India, Tel: +91 08811806866; E-mail: mvenkatasatishkumar@gmail.com

Rec date: June 1, 2017; Acc date: June 21, 2017; Pub date: June 26, 2017

Copyright: © Pradhan S, et al. This is an open-access article distributed under the terms of the Creative Commons Attribution License, which permits unrestricted use, distribution, and reproduction in any medium, provided the original author and source are credited.

Abstract

Graves' disease (GD), an autoimmune disorder, scars majority of women worldwide, causing hyperthyroidism, Graves's ophthalmopathy and goitre. Thyroid Peroxidase (TPO) is an active target of anti-thyroid drugs, Methimazole and Propylthiouracil, which inhibit the enzyme function of catalysing the thyroid hormones synthesis. Most of the protein-drug interaction studies so far have been focussed mainly at *in vivo* level, or by using Myeloperoxidase and Lactose peroxidases as TPO surrogates for the same. This makes the molecular interaction of TPO with the drugs crucial to understand. In this study, we used the molecular dynamics (MD) to study the molecular interaction differences between TPO₂₀₁₋₅₀₀ and both drugs. The binding free energy calculation done using Molecular Mechanics Poisson-Boltzmann (MM-PBSA) and generalized Born and surface area continuum solvation (GBSA) results indicated that both drugs bind strongly to TPO₂₀₁₋₅₀₀, with Propylthiouracil having slightly higher binding energy than Methimazole. We found that both drugs interacted with the residues- Asp238, His239, Phe243, Thr487 and His494 through hydrophobic interactions and formed stable hydrogen bonds with residue Arg491 of TPO₂₀₁₋₅₀₀. Since both drugs engage residues- Asp238, His239 and His494 which falls within the proximal heme binding site and catalytic site of TPO₂₀₁₋₅₀₀, we can conclude that these drugs may be conducive in inhibiting the enzymatic activity of TPO₂₀₁₋₅₀₀.

Keywords: Graves' disease; Thyroid peroxidase; Methimazole; Propylthiouracil; Molecular dynamics; MM-PBSA/GBSA

Introduction

Graves' disease (GD) is an autoimmune Thyroid disorder (AITD), typically characterized by the presence of thyrotoxicosis, goiter, and ophthalmopathy (Grave's ophthalmopathy) [1]. It is one of the major causes of hyperthyroidism in the geographical areas with Iodine abundance [2]. GD has reported a frequency of 20-30 cases per 100,000 individuals each year, with the possibility 3% of women and 0.5% of men acquiring GD during their lifetime [3]. The main ground cause of GD is the binding of circulating IgG antibodies to G-protein-coupled thyrotropin receptor (TSHR), resulting in the activation of Thyroglobulin gene which codes for thyroid hormones- triiodothyronine (T3) and thyroxine (T4) [4,5].

These antibodies are thyroid-stimulating antibodies (TSAbs) [6], - often called TSH receptor autoantibody (TSHRAb or TRAb) [7] that replicates the effect of the TSHR's natural ligand Thyrotropin (TSH) by stimulating cyclic adenosine monophosphate (cAMP)-dependent signal transduction, thereby activating the Thyroglobulin gene present within the thyroid gland [6, 8]. Thyroglobulin gene is naturally activated by hypothalamus upon the binding of TSH to TSHR. Since the activation of Thyroglobulin gene by the binding of TSIs to THSR is not natural, there is no feedback system leading to the excess production of thyroid hormones: triiodothyronine (T3) and thyroxine (T4) that is catalyzed by Thyroid Peroxidase (TPO) [6,9]. This activation also triggers follicular hypertrophy and hyperplasia, thyroid enlargement [4].

The synthesis of triiodothyronine T3 and thyroxine T4 hormones from Thyroglobulin gene is catalyzed by Thyroid Peroxidase (TPO) upon the iodination and coupling of tyrosyl residue in Thyroglobulin [10] and is hence the target site of anti-thyroid drugs for the treatment of GD. TPO₂₀₁₋₅₀₀ is a 933 residues transmembrane homodimer [11-13], affixed to the apical membrane of thyroid follicle cells by its TMD region on its C-terminal end (residues 847-871) [14,15]. The X-ray crystallised structure of TPO was determined 16 years ago, but of low resolution [16,17]. TPO shares 47% homology with eosinophil peroxidase (EPO), 48% with Lactose Peroxidase (LPO), and 47% with myeloperoxidase (MPO) [18,19]. Based on these homology studies, it was found that Asp238, His239, Glu399, and His494 were important for proximal heme linkage. The proximal histidine residues present in heme peroxidases are crucial in the redox properties of heme iron for catalysis [20, 21]. The homology modeling of TPO was done recently, reporting that its cis and trans conformations are involved equally in its antigenicity [22].

The antithyroid drug (ATD), Propyl- thiouracil (6-propyl-2-thiouracil) (PTU) and Methimazole (1-methyl-2-mercaptoimidazole, Tapazole) (MMZ), are prescribed exclusively for controlling the hyperthyroidism in GD [23-26]. Both ATDs obstructs the iodination of tyrosyl residues in Thyroglobulin catalyzed by Thyroid Peroxidase, thereby arresting the production of thyroid hormones [27-29]. MMZ is preferred to PTU, due to its better adherence and bioavailability [23,30-32]; however, PTU is also recommended for pregnant women [33,34]. Irradiation studies too have been done to treat hyperthyroidism [35].

The drug binding mechanism of PTU/MMZ to TPO have only been done in-vivo [36-39], however the molecular insights are yet to be understood. Due to the close homology, LPO has been used as surrogates to study interaction of TPO with anti-Thyroid drug MMZ. MMZ-LPO catalyzed oxidation of 2,2'-azobis(3-ethylbenzothiazoline-6-sulfonic acid) (ABTS) and H₂O₂ was carried out where the turnover was estimated to be ~7.0 IM. [40]. The enzyme inhibition study between LPO- MMZ showed that inhibition occurred at the heme group and side chains Arg255, Glu258, and Leu262 of LPO. Gln105 and His109 of the LPO too were involved in the enzyme inhibition [41].

In this study, we have taken up PTU and MMZ as our drug of choice considering the disease. The protein structure of TPO₂₀₁₋₅₀₀ was constructed first, and its stability was asserted. The complex structures of TPO₂₀₁₋₅₀₀ with both the drugs were constructed using PatchDock server [42,43] which gave the results based on the maximum surface area and minimum atomic contact energy. LigPlot+ software v.1.4.5 [44] was employed to investigate the various bonding and non-bonding interactions between the drugs and TPO₂₀₁₋₅₀₀. Since the residues- Asp238, His239 and His494 belonging to the heme linkage region of the protein TPO were seen to be involved in the bond interaction with both drugs, these sites will now no longer be available for the iodination and coupling of tyrosyl residues by TPO for the synthesis of thyroid hormones. R491 was also found to play crucial role in the drug-protein communication by forming hydrogen bond. Binding energy calculation further confirmed that both drugs possessed high affinity towards TPO₂₀₁₋₅₀₀.

The antechamber [45] module of AMBER12 [46] software package was used for prepping the ATDs prior to the simulation. Each of the TPO₂₀₁₋₅₀₀-ATD complexes was subjected to Molecular Dynamics simulation to study its stabilizing properties. In addition, Poisson-Boltzmann and generalized Born and surface area continuum solvation (MM/PBSA and MM/GBSA) [47-51] techniques were endorsed to calculate binding free energies of MMZ and PTU to TPO₂₀₁₋₅₀₀. PBTOT for TPO₂₀₁₋₅₀₀-MMZ and TPO₂₀₁₋₅₀₀-PTU was -11.05 and -14.02 kcal mol⁻¹ while GBTOT for TPO₂₀₁₋₅₀₀-MMZ and TPO₂₀₁₋₅₀₀-PTU was found -9.43 and -15.47 kcal mol⁻¹ respectively, which put forth the inhibitors to have high affinity to TPO₂₀₁₋₅₀₀ in the dynamic system. Our findings affirm that both the drugs are equally effective as an anti-thyroid drug. Moreover, our results may further provide guidance to developing more potent inhibitors of TPO and preventing thyroid hormone production in GD.

Materials and Methods

Computational model

The amino acid sequences were obtained from UniProt [52], ID No. P07202 by querying the TPO₂₀₁₋₅₀₀ protein sequence against RCSB PDB web server [53, 54] domain of Thyroid Peroxidase protein sequence (residues 201-500) was submitted to Iterative Threading ASSEMBLY Refinement server (ITASSER) [55-57] for the 3D structure prediction. From I-TASSER we obtained 5 best models ranked according to their C-scores out of which best model is chosen based on C-score, Template Modelling (TM) score [58] and Root Mean Square Deviation (RMSD) score. Using RAMPAGE [59] and VERIFY 3D server [60,61] we validated the structure of TPO₂₀₁₋₅₀₀.

Based upon the 3D structural validation checks, Model 1 showed consistently good results among the rest, hence chosen as an ideal

structure of TPO₂₀₁₋₅₀₀ for further studies. SOPMA (Self-optimized prediction method alignment) server [62] was adopted in studying the secondary structure of TPO₂₀₁₋₅₀₀. Anti-thyroid drug: Propylthiouracil (PTU) and Methimazole (MMZ/MMI) were chosen for this study. 3D conformer of both the ATDs were procured from PubChem server [63] in SDF format, which was later converted to pdb file using open Babel software v.2.3.2 [64].

Docking

The initially constructed 3D structures of TPO₂₀₁₋₅₀₀ with PTU and MMZ were processed separately for the rigid molecular docking using the PatchDock [42,43] web server. PatchDock works on the principle of geometric surface docking algorithm. The clustering score of 1.5 Å RMSD was given to remove the unwanted models. The ten complexes of TPO₂₀₁₋₅₀₀-PTU and TPO₂₀₁₋₅₀₀-MMZ were obtained from the server. Based on highest surface area and lowest atomic contact energy, one complex each of TPO₂₀₁₋₅₀₀-MMZ and TPO₂₀₁₋₅₀₀-PTU were selected.

Determining interacting residues and bond types

The best structure of TPO₂₀₁₋₅₀₀ in complex with PTU and MMZ processed by PatchDock was selected among the rest considering the minimum atomic contact energy and maximum surface area. The best structure was visualized in LigPlot+ software v.1.4.5 [44] for evaluating the interacting residues of TPO₂₀₁₋₅₀₀ interacting with the drugs. Interface residues are defined as the residues with a contact distance less than 6 Å from the interacting partner.

Molecular dynamics simulations of thyroid peroxidase (TPO₂₀₁₋₅₀₀) with anti-thyroid drugs (ATD) - methimazole and propylthiouracil

The molecular dynamics study was performed using AMBER12 [46] software package where ff99SB force field [65] parameters were used for protein (TPO₂₀₁₋₅₀₀) and generalized AMBER force field (GAFF) [66] parameters of the anti-thyroid drugs-Methimazole and Propylthiouracil were established with the Antechamber [45] program, wherein AM1-BCC [67,68] was used to fix the proportionate partial atomic charges. Using xLEaP and antechamber module in AMBER12, we prepared the initial coordinate and the topology files for two the complex systems.

Xleap also added all the missing parameters to the complexes. All the canonical systems were then neutralized with Na⁺ ions, followed by the hydration with TIP3P [69] water molecules in a box with a buer size of 10 from the solute in x, y, and z axis. The initial minimization of the solvated structures was done imposing the constraints over the solute for the first 500 steps using the steepest descent algorithm followed by another 500 steps with a conjugate gradient method. Second minimization was carried out freely for 500 steps. 8 Å was applied as the cut off for both the minimization steps. Gradual heating was done to both the complexes with the successive increase in the temperature from 0-300K. The generated ensemble was then equilibrated for 100ps using the NPT ensemble at 300 K and 1 atmospheric pressure. Full MD production run was carried out till 15ns.

Periodic boundary conditions along with all the electrostatic interactions were maintained throughout the simulations using the particle mesh Ewald (PME) method [70,71] under isothermal and

isobaric conditions respectively. The temperature was governed using Berendsen thermostat [72]. The production run was attained with the NPT ensemble for all the formerly mentioned Thyroid Peroxidase-Anti thyroid drug complexes for 15 ns with 2 fs time step. Furthermore, the shake algorithm [73] was used to restrain all the bonds including the hydrogen atoms.

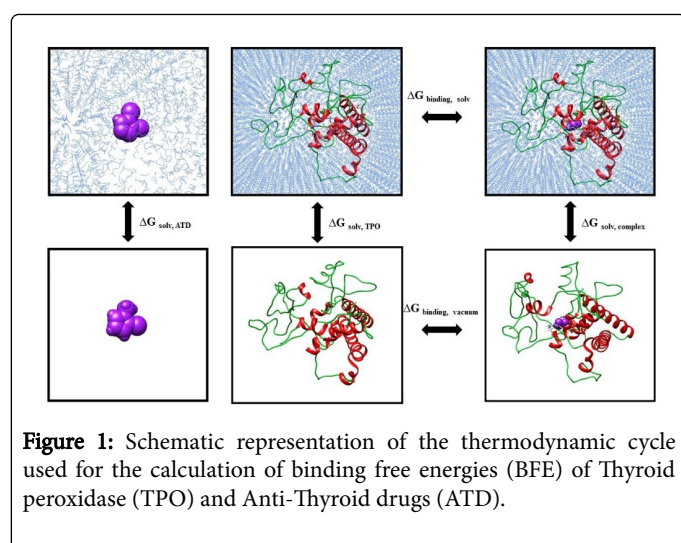
MD analyses

To check the stability of the obtained MD trajectories, each trajectory were clustered to acquire comparative Root Mean Square Deviation (RMSD), Radius of Gyration (Rg), B-factor and Solvent Accessible Surface Area (SASA) using the CPPTRAJ algorithm [74] of Amber12 package. We also proceeded further to analyze hydrogen bond properties based on all possible hydrogen donors (HD) and acceptors (HA) in the system, the percentage occupancy of hydrogen during each step of MD trajectory and considering bond distances and bond angle made by HA-H-HD atoms. Here, the hydrogen bonds having consistency for more than 5% of the simulation period were taken as an output result. Molecular graphics and analyses of the trajectories obtained were performed using UCSF Chimera package [75] and VMD v.1.9.3 [76].

Binding Free Energy (BFE) calculations

The binding free energy between the protein and the drugs were assessed by considering the thermodynamics pattern of Figure 1. The binding free energies of two anti-thyroid drugs- Methimazole and Propylthiouracil to Thyroid peroxidase were computed using MM-GBSA (Molecular Mechanics Generalized Born Surface Area) and MM-PBSA (Molecular Mechanics Poisson-Boltzmann Surface Area approach [47-51] in AMBER program. We took 100 conformational snapshots extracted from the last 1 ns of MD trajectories. Independent MM-GBSA/PBSA analysis was done for (i) Thyroid peroxidase (TPO₂₀₁₋₅₀₀) (ii) anti-thyroid drugs (ATD) - MMZ/PTU and (iii) the complex- TPO₂₀₁₋₅₀₀-MMZ/PTU. The binding free energies of TPO₂₀₁₋₅₀₀ with both the drugs were calculated using equation 1.

$$\Delta G_{\text{binding}} = \Delta G_{\text{complex}} - [\Delta G_{\text{TPO}} + \Delta G_{\text{ATD}}] \quad (1)$$



Where G_{binding} corresponds to the total binding free energy, G_{complex} , G_{TPO} and G_{ATD} are the solvation free energies of the complex, thyroid peroxidase and anti-thyroid drugs, respectively. BFE

as stated by second law of thermodynamics can also be summed as the difference between enthalpy ΔH and the conformational entropy $-T\Delta S$ [48,51] of the system which can be represented by the equation 2.

$$\Delta G_{\text{binding}} = \Delta H - T\Delta S \quad (2)$$

ΔH can be explained as sum of the changes of the gas-phase molecular mechanics energies (ΔE_{MM}), polar and non-polar solvation energy (ΔG_{solv}); see equation 3. Also, ΔE_{MM} is the sum total, of the differences in the bond, angle and dihedral energies ($\Delta E_{\text{internal}}$), van der Waals (ΔE_{vdW}), and electrostatic energies (ΔE_{ele}), as shown in the equation 4. Accordingly, equation 5 divides ΔG_{solv} into polar ($\Delta G_{\text{PB/GB}}$) and non-polar solvation free energy (ΔG_{surf});

$$\Delta H = \Delta E_{\text{MM}} + \Delta G_{\text{solv}} \quad (3)$$

$$\Delta E_{\text{MM}} = \Delta E_{\text{internal}} + \Delta E_{\text{vdW}} + \Delta E_{\text{ele}} \quad (4)$$

$$\Delta G_{\text{solv}} = \Delta G_{\text{PB/GB}} + \Delta G_{\text{surf}} \quad (5)$$

The terms E_{int} , E_{vdW} , and E_{ele} are internal energy, van der Waals interaction, and electrostatic interaction of the systems respectively. The terms $\Delta G_{\text{PB/GB}}$ and ΔG_{surf} are polar and non-polar solvation free energies. The modified GB model of Onufriev [77] was considered in the determination of the ΔG_{GB} . A value of 80 was considered for the internal dielectric constant of the solvent (water) while, the external dielectric constant of the solute was set to 1. The non-polar solvation free energy (ΔG_{surf}) for both the systems was estimated equation 6.

$$\Delta G_{\text{surf}} = \gamma \times \text{SASA} + \beta \quad (6)$$

Where SASA is the abbreviation of solvent-accessible surface-area. In case of PB method, γ was to 0.00542 kcal (mol⁻¹ Å⁻²) and $\beta = 0.92$ kcal mol⁻¹, while for the GB method, γ was customized to 0.0072 kcal (mol⁻¹ Å⁻²) and $\beta = 0$ kcal mol⁻¹ respectively [78]. 1.4 Å was the probe radius of the solvent used for these calculations.

Results and Discussion

Structural modelling and validation of thyroid peroxidase

We modelled the structure of Thyroid Peroxidase (TPO₂₀₁₋₅₀₀) from I-TASSER (Figure 2). The server provided us with five models using the threading algorithm. The ideal model was selected based upon the C-score computed from the comparative structural significance. The C-score for TPO₂₀₁₋₅₀₀ was 1.20. The overall quality of model was achieved by various bioinformatics tools. TM scored TPO₂₀₁₋₅₀₀ in the rage of 0.88 ± 0.07 and RMSD estimated was 3.8 ± 2.6 Å. The structural justification of the ITASSER yielded structure was done by RAMPAGE server. We observed 81.5% of residues were within most favored region, 11.4% in allowed region and 7.0% in disallowed region. Verify-3D server ascertains the accuracy of the predicted secondary structure (3D) model with its respective residues (1D) by assigning a structural class based on its location and environment. 81.6% of residues had an averaged 3D-1D score ≥ 0.2 which confirms the accuracy of the predicted model to near correct to the actual structure. SOPMA server identified 39.33% α -helices, 47.67% random coil, 7.33% or extended strand and 5.67% of β -strands respectively in the modeled structure of Thyroid Peroxidase.

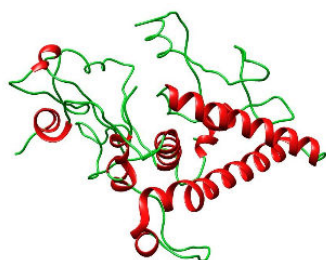


Figure 2: Modelled structure of Thyroid Peroxidase (TPO) obtained from ITASSER server with the C-score of 1.20.

Protein-drug interaction study

It is an evident fact that Methimazole and Propylthiouracil interferes in the synthesis of thyroid hormones by regulating the enzyme inhibition of thyroid peroxidase. The in-vivo/in-vitro binding mechanisms of PTU/MMZ to TPO₂₀₁₋₅₀₀ have also been done exclusively, yet the interactions at the molecular level are not known. So as to understand the drug-protein interaction at the molecular stage, we docked Thyroid peroxidase with both the drugs using PatchDock, server. This particular server works on the principle of geometric hashing which is implied as a best molecular shape complementarity between the docked structures considering the wide interface area and lesser steric hindrances. The docking gave us array of docked structures for TPO₂₀₁₋₅₀₀-MMZ/PTU complex. These complexes were graded basis of geometric shape, interface area and atomic contact energy as shown in Figures 3 and 4. The best ranked structure in case of TPO₂₀₁₋₅₀₀-MMZ complex had a geometric shape complementarity score of 2300, approximate interface area of 260.2 Å² and atomic contact energy of (ACE) of -152.3 kcal mol⁻¹ (Solution Structure 1 from Figure 3). Likewise, the top scored structure for TPO₂₀₁₋₅₀₀-PTU was found to have the geometric score of 2912, interface area of about of 328.8 Å² and ACE of -146.6kcal mol⁻¹ (Solution Structure 1 from Figure 4).

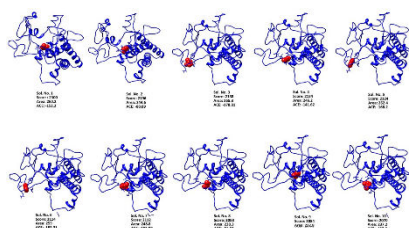


Figure 3: Docked structures of thyroid peroxidase-methimazole (MMZ) obtained from patchdock server.

Next, we examined the hydrogen and hydrophobic interaction occurring in protein-drug complex using the Ligplot+ tool as shown in Figures 5A and 5B. Figure 5A details the interaction between Thyroid Peroxidase and Methimazole. Arg491 formed a hydrogen bond with the thiol atom i.e., Sulphur at the distance of 3.25 Å. Hydrophobic bonds are formed between the protein and the drug by residues Asp238, His239, Phe243, Thr487 and His494. Figure 5B showcases the molecular interaction between TPO₂₀₁₋₅₀₀ and Propylthiouracil. We

can clearly observe the hydrogen bond formed between residue Arg491 and Sulphur atom of the drug PTU at the distance of 3.04 Å. Amino acids Asp238, Gln235, His239, Phe243, Glu399, Thr487 and His494 formed the hydrophobic bonds with the drug. In both the scenarios, drug is seen to have bonded with proximal heme binding residues of the protein- Asp238, His239 and His494.

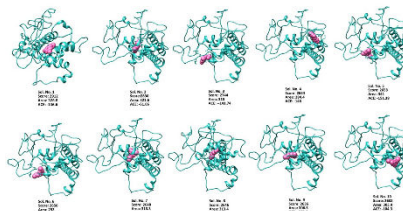


Figure 4: Docked structures of thyroid peroxidase and propylthiouracil (PTU) obtained from patchdock server.

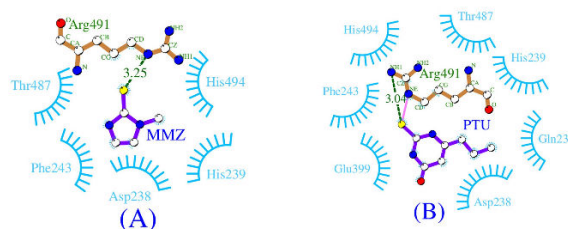


Figure 5: LIGPLOT representation of Anti-Thyroid drugs-Methimazole (MMZ) and Propylthiouracil (PTU) binding to Thyroid Peroxidase (TPO). Ligand, protein, and hydrogen bonds are in thick purple, thick brown and green dash lines, respectively. Hydrophobic contacts forming residues are shown in sky blue colour as an arc with spikes towards ligand atoms (A) Thyroid Peroxidase (TPO) bound to Methimazole (MMZ). (B) Thyroid Peroxidase (TPO) bound to Propylthiouracil (PTU).

Since these residues are bound to the drug, which renders the active site of the protein unavailable for its ritual catalyzing activity thereby inhibiting the production of the thyroid hormones. Another homolog study of TPO was done in LPO by Singh et al., where they found that the heme moiety residues held MMZ tightly on one side while hydrophobic amino acids - Arg255, Glu258, and Leu262 held it on the other end. Many extensive studies on LPO as TPO surrogate has supported the importance of heme binding and catalytic site residues mainly Hisidines and Aspartic acid in mammalian peroxidases [79-81]. A review on MPO highlighted its ligand binding site to be present within the distal heme pocket which upon the binding of PTU, isoniazid could lead to irreversible inactivation of the enzyme [82]. The homology studies done by Taugog in 1999 and Furtmüller et al. have pointed out the essentiality of the proximal histidine residues for the prime functioning of TPO₂₀₁₋₅₀₀ to catalyse the iodination of tyroysl

residues in thyroglobulin. And we have noted these histidine residues His239 and His494 to have been engaged by anti-thyroid drugs due to hydrophobic linkage, also relieving the protein of its catalytic role. Comparative study on the effective dosage of Methimazole and Propylthiouracil in Patients with GD by Nakamura et al. [83] revealed that 15 mg/d of MMI is prescribed for mild and moderate GD, 30 mg/d of PTU is recommended for severe forms of GD. A team of scientists from Spain and Argentina [84] determined the pharmacological activities of a copper based propylthiouracil ($[\text{Cu}(\text{PTU})_2]_2$), and concluded that this combination of PTU would be good candidate due to its antioxidant, antimicrobial and alkaline phosphatase activity.

MD simulation study on the TPO₂₀₁₋₅₀₀-MMZ/PTU complex

The molecular dynamics simulations were administered to probe the efficacy of both the anti-thyroid drugs- Methimazole and Propylthiouracil as an inhibitor for thyroid peroxidase. Extracting the trajectory output, we analyzed the stability of TPO₂₀₁₋₅₀₀-MMZ/PTU complexes in an explicit environment. The conformational dynamics of TPO₂₀₁₋₅₀₀ complexed with the drugs-MMZ and PTU were estimated by plotting the Root Mean Square Deviation (RMSD) by taking their respective equilibrated structures as a reference. The comparative RMSD graph for the C α atoms of the TPO₂₀₁₋₅₀₀-MMZ/PTU complexes as a function of time can be seen in Figure 6A. MMZ bound TPO₂₀₁₋₅₀₀ started to settle at the RMSD value of around 5 Å while MMZ bound XPA was exhibiting fluctuations even at the RMSD value of ~ 7.5 Å. The stability of PTU over MMZ in the biological system can also be explained from the study done by Yoshihara et al., where they found that over exposure of the in utero foetus to MMZ increased the risks of congenital malformations and least with PTU prescriptions.

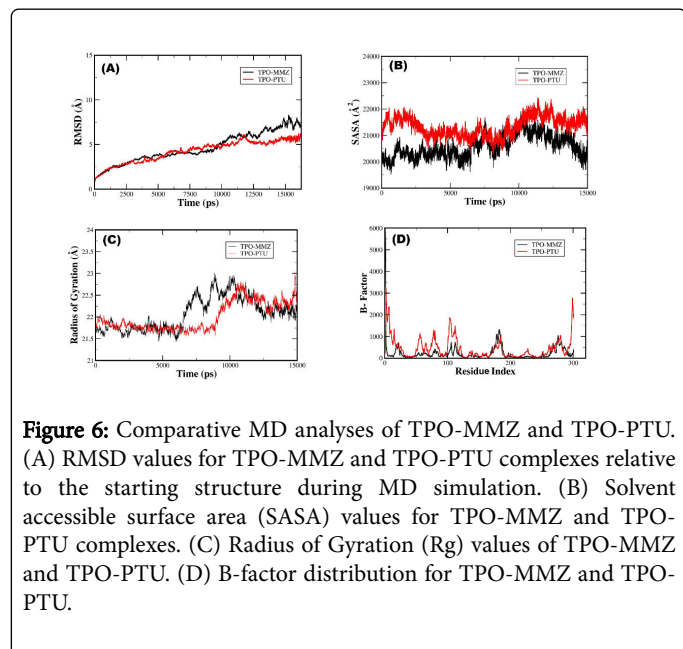


Figure 6: Comparative MD analyses of TPO-MMZ and TPO-PTU. (A) RMSD values for TPO-MMZ and TPO-PTU complexes relative to the starting structure during MD simulation. (B) Solvent accessible surface area (SASA) values for TPO-MMZ and TPO-PTU complexes. (C) Radius of Gyration (Rg) values of TPO-MMZ and TPO-PTU. (D) B-factor distribution for TPO-MMZ and TPO-PTU.

Figure 6B shows the solvent accessible surface area (SASA) for the both the protein-drug complexes. Both the systems, be it TPO₂₀₁₋₅₀₀-MMZ or TPO₂₀₁₋₅₀₀-PTU had proper access to the solvent provided in the water box throughout the simulation. TPO₂₀₁₋₅₀₀-MMZ presented the SASA value of within 20000-22000 Å² while PTU-showed SASA

value in the range of 21000-22500 Å². TPO₂₀₁₋₅₀₀-PTU complex required much larger surface area to access the solvent in the system.

We determined the comparative radius of gyration (Rg) for both the drugs complexed with TPO₂₀₁₋₅₀₀. Rg quantifies the compactness and the spatial dispersal of the atoms, of a particular component molecule, around an axis. Figure 6C shows the radius of gyration for TPO₂₀₁₋₅₀₀ bound to Methimazole and Propylthiouracil as a function of time. Methimazole bound TPO₂₀₁₋₅₀₀ showed oscillations from 6 ns onwards, while TPO₂₀₁₋₅₀₀-PTU was settled till 9 ns, then it started oscillating.

Next, we analyzed B-factor graph for the backbone C α -atoms for the TPO₂₀₁₋₅₀₀ in complex with both the drugs to observe the variations in their structural dynamics from their average position. Figure 6D shows that both the systems presented more or less coherent atomic fluctuations, and the only difference between them being the higher peaks as seen in the TPO₂₀₁₋₅₀₀-PTU complex, whereas TPO₂₀₁₋₅₀₀-MMZ had shorter peaks meaning less atomic fluctuations.

Hydrogen bond analysis as seen in Figure 7 showed intermolecular hydrogen bonds formed between the enzyme and the drug during the simulation period. As per Figure 7A, we saw two hydrogen bonds formation in TPO₂₀₁₋₅₀₀-PTU complex form, while only single hydrogen bond formed in case of TPO₂₀₁₋₅₀₀-MMZ (Figure 7B) during simulation. We further calculated the inter-molecular hydrogen bond stability of both the systems.

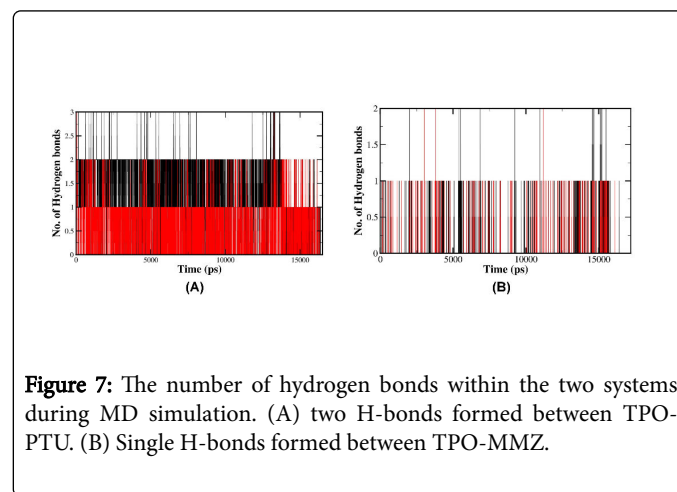


Figure 7: The number of hydrogen bonds within the two systems during MD simulation. (A) two H-bonds formed between TPO-PTU. (B) Single H-bonds formed between TPO-MMZ.

Table 1 shows hydrogen bond occupancy of the inter-molecular hydrogen bonds formation as the function of time period. We found the important amino acids Arg491 had high fraction of occupancy in the complex of TPO₂₀₁₋₅₀₀-MMZ while Asp238 and Phe485 had greater fractions for hydrogen bond formation in case of TPO₂₀₁₋₅₀₀-PTU. Higher fraction of hydrogen bond definitely suggested the stronger interaction between the protein TPO₂₀₁₋₅₀₀ and the ATDs. These occupancies align exactly with the Figures 7A and 7B for the total number of the hydrogen bonds formed within the systems. We simultaneously took comparative snapshots of both the TPO₂₀₁₋₅₀₀-MMZ and TPO₂₀₁₋₅₀₀-PTU systems at different intervals of simulation period and are presented in Figure 8.

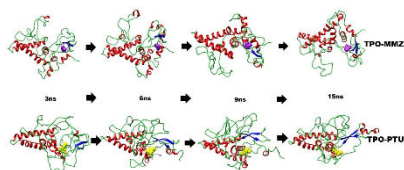


Figure 8: Comparative snapshots for TPO-MMZ and TPO-PTU at 3 ns, 6 ns, 9 ns and 15 ns respectively.

Both the systems presented the β -sheets formations. PTU bound TPO₂₀₁₋₅₀₀ had loss of the α -helices over the simulation period.

Anti-Thyroid drugs	Atoms of Hydrogens bonds	Fractions
Methimazole (MMZ)	N1:LIG- HG2:ARG491	0.6100
	N1:LIG- O:CYS269	0.057
	N1:LIG- OE1: GLN316	0.0021
	N1:LIG- O:THR487	0.0021
	N1:LIG- CE2:PHE270	0.0012
Propylthiouracil (PTU)	N:LIG- OD1:ASP238	0.5346
	N1:LIG- O:PHE485	0.503
	N1:LIG- O:THR244	0.097
	N1:LIG- O:ALA489	0.0446
	N1:LIG-O:SER486	0.0093

Table 1: H-bond occupancy among all MD simulations.

Calculations of binding free energies

To measure the efficacy of the anti-thyroid drugs- Methimazole and Propylthiouracil in inhibiting the enzyme activity of Thyroid peroxidase in Graves' disease, the binding free energies were evaluated using MM-PBSA/GBSA method as provided in AMBER program. The calculated values are summarized in Table 2. According to Table 2, the binding free energy of the TPO₂₀₁₋₅₀₀-MMZ complex using MM-PB/GBSA methods is found to be -11.05 (PBTOT) and -9.43 (GBTOT) kcal mol⁻¹. TPO₂₀₁₋₅₀₀-PTU complex had the binding free energy of -14.02 (PBTOT) and -15.47 (GBTOT) kcal mol⁻¹. As per the data obtained, the drug-protein binding was considerably enhanced by the contributions of the van der Waals interactions (ΔE_{vdW}), non-polar solvation energy (ΔG_{surf}) and electrostatic interactions (ΔG_{ele}).

Method	Contribution	Complexes	
		TPO-MMZ (kcal mol ⁻¹)	TPO-PTU (kcal mol ⁻¹)
MM	ELE	-16.90 \pm 4.46	-13.45 \pm 3.61
	VDW	-12.48 \pm 1.78	-21.62 \pm 1.25
	INT	0	0

	GAS	-29.38 \pm 4.30	-35.08 \pm 3.09
	PBSOR	-1.53 \pm 0.05	-2.13 \pm 0.11
PBSA	PBCAL	19.86 \pm 3.67	23.18 \pm 2.19
	PBSOL	18.33 \pm 3.69	21.05 \pm 2.22
	PBELE	2.96 \pm 1.62	9.73 \pm 2.56
	PBTOT	-11.05 \pm 1.81	-14.02 \pm 2.09
	GBSURF	-1.53 \pm 0.05	-2.21 \pm 0.11
GBSA	GB	21.48 \pm 3.62	21.73 \pm 2.73
	GBSOL	19.95 \pm 3.64	19.60 \pm 2.80
	GBELE	4.59 \pm 1.30	8.28 \pm 1.36
	GBTOT	-9.43 \pm 1.26	-15.47 \pm 1.24

ELE: Electrostatic energy as calculated by the MM force field,
VDW = Van der Waals contribution from MM,
INT = Internal energy arising from bond, angle, and dihedral terms in the MM force field. (This term always amounts to zero in the single trajectory approach),
GAS = Total gas phase energy (sum of ELE, VDW, and INT),
PBSUR/GBSUR = Non-polar contribution to the solvation free energy calculated by an empirical model.
PBCAL/GB = The electrostatic contribution to the solvation free energy calculated by PB or GB, respectively.
PBSOL/GBSOL = Sum of non-polar and polar contributions to solvation,
PBELE/GBELE = Sum of the electrostatic solvation free energy and MM electrostatic energy, **PBTOT/GBTOT** = Final estimated binding free energy in kcal mol⁻¹ calculated from the terms above.

Table 2: Binding free energies (kcal mol⁻¹) between Thyroid peroxidase (TPO) and Anti-Thyroid drugs- Methimazole (MMZ) and Propylthiouracil (PTU).

The PBTOT or GBTOT values of both the complexes showed not much difference in their overall binding energy. For PBTOT, the differences were 14.02-11.05 = 2.97 kcal mol⁻¹, while their GBTOT difference was however quite large i.e., 15.47-9.43 = 6.04 kcal mol⁻¹. Based on these results, Propylthiouracil showed better results in enzyme inhibition than Methimazole. Nonetheless, both the drugs are equally qualified in target binding of Thyroid peroxidase and thereby preventing the production of thyroid hormones. A population study conducted by Azizi and his team in 2014 for the management of hyperthyroidism in Asia too showed the preference of PTU over MMZ by the clinician's due to its better outcome. A density functional theory method was opted by Tappa and his group [85] to evaluate the inhibitory effect of the MMZ tautomers-1-methyl-1H-imidazole-2(3H)-thione (M1) and 1-methyl-1H-imidazole-2-thiol (M2) where the effect of M1 was superior to M2 tautomer. Gupta and Kumar [86] did metabolic modelling and tested the drug activity of PTU against TPO, TSHR and sodium iodide symporter (NIS) using systems biology approach and deduced that PTU is effective on TPO. They also observed TSHR to be potent target for therapeutic study. A study done on PTU, KClO₄, or TSH [87] revealed that these compounds reduced the oxidative stress due to high concentrations of iodide in the thyroids of both Metallothioneins(MTs) MT-I/II KO and WT mice. Bhabak and Mughesh in 2010 [88], and Manna, Roy and Mughesh in 2013 [89], reported Selenium analogues of ATDs to have better inhibitory effect

compared to Sulphur based thionamide drugs on TPO suggesting that this selenium based drugs may be the next potential ATDs.

Conclusion

In this computational study, the protein structure of thyroid peroxidase was modelled first, followed by the independent docking of the protein with MMZ and PTU. We have identified the residues that are involved in the drug-protein interaction. Both the drugs engaged the heme linkage active site residues- Asp238, His239 and His494, depleting the protein of its function to catalyze the iodination of tyrosyl residues on thyroglobulin for T3 and T4 hormone production. The hydrophobic interaction with residues Asp238, His239, Phe243, Thr487 and His494 was seen in both the cases. Proximal histidine residues His239 and His494 were also found to be interacting with the drug making the enzyme unfit to carry out its biological role. Arg491 was also found to be binding with the drug by hydrogen bonding. RMSD showed the stability of MMZ to be much higher than PTU. TPO₂₀₁₋₅₀₀-PTU had higher values for SASA and B-factor graphs. Hydrogen bond analyses too substantiated the stronger and stable interaction shared by these anti-thyroid drugs to the enzyme. MM-PBSA/GBSA binding free energy results showed both drugs to be equipped in binding to TPO₂₀₁₋₅₀₀ and in inhibiting the catalytic activity of TPO₂₀₁₋₅₀₀ in thyroid hormone synthesis as seen in the literatures. Propylthiouracil showed comparatively higher binding efficiency than methimazole as per GBTOT analysis, yet there was not much difference between their binding energies considering the PBTOT results. After studying all the obtained evidences, we deduce that both the anti-thyroid drugs are competent enough to inhibit the enzyme activity of Thyroid peroxidase, and in process keeping the unwanted production of thyroid hormone at bay.

Acknowledgements

The authors extend their deepest gratitude towards Tezpur University for the start-up grant. This research was also supported by Department of Biotechnology (DBT) funded Bioinformatics Infrastructure facility (BIF) in the Department of Molecular Biology and Biotechnology at Tezpur University.

References

1. Menconi F, Marcocci C, Marinò M (2014) Diagnosis and classification of Graves' disease. *Autoimmun Rev* 13: 398-402.
2. Bartalena L, Burch HB, Burman KD, Kahaly GJ (2016) A 2013 European survey of clinical practice patterns in the management of Graves' disease. *J Clin Endocrinol Metab* 84: 115-120.
3. Burch HB, Cooper DS (2015) Management of Graves' disease: A review. *JAMA* 314: 2544-2554.
4. Brent GA (2008) Graves' disease. *N Engl J Med* 358: 2594-2605.
5. Sanders J, Chirgadze DY, Sanders P, Baker S, Sullivan A, et al. (2007) Crystal structure of the TSH receptor in complex with a thyroid-stimulating autoantibody. *Thyroid* 17: 395-410.
6. Swain M, Swain T, Mohanty BK (2005) Autoimmune thyroid disorders—An update. *Indian J Clin Biochem* 20: 9-17.
7. Orgiazzi J (2000) Anti-Tsh Receptor Antibodies in Clinical Practice. *Endocrinol Metab Clin North Am* 29: 339-355.
8. Leschik JJ, Diana T, Olivo PD, König J, Krahn, U, et al. (2013) Analytical performance and clinical utility of a bioassay for thyroid-stimulating immunoglobulins. *Am J Clin Pathol* 139: 192-200.
9. Hashizume K, Ichikawa K, Sakurai A, Suzuki S, Takeda T, et al. (1991) Administration of thyroxine in treated Graves' disease: effects on the level of antibodies to thyroid-stimulating hormone receptors and on the risk of recurrence of hyperthyroidism. *N Engl J Med* 324: 947-953.
10. Taugo A, Dorris ML, Doerge DR (1996) Mechanism of simultaneous iodination and coupling catalyzed by thyroid peroxidase. *Arch Biochem Biophys* 330: 24-32.
11. Baker Jr JR, Arscott P, Johnson J (1994) An analysis of the structure and antigenicity of different forms of human thyroid peroxidase. *Thyroid* 4: 173-178.
12. Kimura S, Kotani T, McBride OW, Umeki K, Hirai K, et al. (1987) Human thyroid peroxidase: complete cDNA and protein sequence, chromosome mapping, and identification of two alternately spliced mRNAs. *Proc Natl Acad Sci* 84: 5555-5559.
13. McDonald DO, Pearce SH (2009) Thyroid peroxidase forms thionamide-sensitive homodimers: relevance for immunomodulation of thyroid autoimmunity. *J Mol Med* 87: 971-980.
14. Kimura S, Ikeda-Saito M (1988) Human myeloperoxidase and thyroid peroxidase, two enzymes with separate and distinct physiological functions, are evolutionarily related members of the same gene family. *Protein Struct Funct Genet* 3: 113-120.
15. Yokoyama N, Taugo A (1988) Porcine thyroid peroxidase: relationship between the native enzyme and an active, highly purified tryptic fragment. *Mol Endocrinol* 2: 838-844.
16. Gardas A, Sohi MK, Sutton BJ, McGregor AM, Banga JP (1997) Purification and crystallisation of the autoantigen thyroid peroxidase from human Graves' thyroid tissue. *Biochemical and biophysical research communications* 234: 366-370.
17. Hendry E, Taylor G, Ziemnicka K, Jones FG, Furmaniak, J, et al. (1999) Recombinant human thyroid peroxidase expressed in insect cells is soluble at high concentrations and forms diffracting crystals. *J Endocrinol* 160: R13-R15.
18. Singh AK, Singh N, Sharma S, Singh SB, Kaur P, et al. (2008) Crystal structure of lactoperoxidase at 2.4 Å resolution. *J Mol Biol* 376: 1060-1075.
19. Fiedler TJ, Davey CA, Fenna RE (2000) X-ray crystal structure and characterization of halide-binding sites of human myeloperoxidase at 1.8 Å resolution. *J Biol Chem* 275(16): 11964-11971.
20. Furtmüller PG, Zederbauer M, Jantschko W, Helm J, Bogner M, et al. (2006) Active site structure and catalytic mechanisms of human peroxidases. *Arch Biochem Biophys* 445:199-213.
21. Taugo A (1999) Molecular evolution of thyroid peroxidase. *Biochimie* 81: 557-562.
22. Le SN, Porebski BT, McCoe J, Fodor J, Riley B, et al. (2015) Modelling of Thyroid Peroxidase Reveals Insights into Its Enzyme Function and Autoantigenicity. *PloS one* 10: e0142615.
23. Cooper DS (2005) Antithyroid drugs. *N Engl J Med* 352: 905-917.
24. Burch HB, Burman KD, Cooper DS (2012) A 2011 survey of clinical practice patterns in the management of Graves' disease. *J Clin Endocrinol Metab* 97: 4549-4558.
25. Azizi F, Amouzegar A, Mehran L, Alamdari S, Subekti I, et al. (2014) Management of hyperthyroidism during pregnancy in Asia. *Endocr J* 61(8):751-758.
26. Yoshihara A, Noh J, Yamaguchi T, Ohye H, Sato S, et al. (2012) Treatment of Graves'disease with Antithyroid drugs in the First trimester of pregnancy and the prevalence of congenital malformation. *J Clin Endocrinol Metab* 97: 2396-2403.
27. Solomon B, Glinoe D, Lagasse R, Wartofsky L (1990) Current trends in the management of Graves' disease. *J Clin Endocrinol Metab* 70: 1518-1524.
28. Davidson B, Soodak M, Neary JT, Strout HV, Kieffer JD, et al. (1978) The irreversible inactivation of thyroid peroxidase by methylmercaptoimidazole, thiouracil, and propylthiouracil in vitro and its relationship to in vivo findings. *Endocrinology* 103: 871-882.
29. Garcia-Mayor VR, Larranaga A (2010) Treatment of Graves' hyperthyroidism with thionamides-derived drugs: review. *J Med Chem* 6: 239-246.

30. Nicholas WC, Fischer RG, Stevenson RA, Bass JD (1995) Single daily dose of methimazole compared to every 8 hours propylthiouracil in the treatment of hyperthyroidism. *South Med J* 88: 973-976.
31. Homsanit M, Sriussadaporn S, Vannasaeng S, Peerapatdit T, Nitiyanant W, et al. (2001) Efficacy of single daily dosage of methimazole vs. propylthiouracil in the induction of euthyroidism. *J Clin Endocrinol Metab* 54: 385-390.
32. He CT, Hsieh AT, Pei D, Hung YJ, Wu LY, et al. (2004) Comparison of single daily dose of methimazole and propylthiouracil in the treatment of Graves' hyperthyroidism. *J Clin Endocrinol Metab* 60: 676-681.
33. Hackmon R, Blichowski M, Koren G (2012) Motherisk rounds: The safety of methimazole and propylthiouracil in pregnancy: A systematic review. *J Obstet Gynaecol Can* 34: 1077-1086.
34. Inoue M, Arata N, Koren G, Ito S (2009) Hyperthyroidism during pregnancy. *Can Fam Physician* 55(7): 701-703.
35. Alcaraz M, Solano F, Vicente V, Canteras M (2003) Effect of radiation on thyroid peroxidase activity in rabbit. *Radiobiologia* 3: 59-62.
36. Sugawara M, Sugawara Y, Wen K (1999) Methimazole and propylthiouracil increase cellular thyroid peroxidase activity and thyroid peroxidase mRNA in cultured porcine thyroid follicles. *Thyroid* 9: 513-518.
37. Motonaga K, Ota M, Odawara K, Saito S, Welsch F (2016) A comparison of potency differences among thyroid peroxidase (TPO) inhibitors to induce developmental toxicity and other thyroid gland-linked toxicities in humans and rats. *Regul Toxicol Pharmacol* 80: 283-290.
38. Homsanit M, Sriussadaporn S, Vannasaeng S, Peerapatdit T, Nitiyanant W, et al. (2001) Efficacy of single daily dosage of methimazole vs. propylthiouracil in the induction of euthyroidism. *J Clin Endocrinol Metab* 54: 385-390.
39. Wing DA, Millar LK, Koonings PP, Montoro MN, Mestman JH (1994) A comparison of propylthiouracil versus methimazole in the treatment of hyperthyroidism in pregnancy. *Am J Obstet Gynecol* 170: 90-95.
40. Roy G, Muges G (2006) Bioinorganic chemistry in thyroid gland: effect of anti-thyroid drugs on peroxidase-catalyzed oxidation and iodination reactions. *Bioinorg Chem Appl* 2006: 1-9.
41. Singh RP, Singh A, Sirohi HV, Singh AK, Kaur P, et al. (2016) Dual binding mode of antithyroid drug methimazole to mammalian heme peroxidases—structural determination of the lactoperoxidase-methimazole complex at 1.97 Å resolution. *FEBS open bio* 6: 640-650.
42. Duhovny D, Nussinov R, Wolfson HJ (2002) Efficient unbound docking of rigid molecules. In *International Workshop on Algorithms in Bioinformatics*. Springer Berlin Heidelberg: 185-200.
43. Schneidman-Duhovny D, Inbar Y, Nussinov R, Wolfson HJ (2005) PatchDock and SymmDock: servers for rigid and symmetric docking. *Nucleic Acids Res* 33: W363-W367.
44. Laskowski RA, Swindells MB (2011) LigPlot+: Multiple ligand-protein interaction diagrams for drug discovery. *J Chem Inf Model* 51: 2778-2786.
45. Wang J, Wang W, Kollman PA, Case DA (2006) Automatic atom type and bond type perception in molecular mechanical calculations. *J Mol Graph Model* 25: 247-260.
46. Case DA, Darden TA, Cheatham TE, Simmerling CL, Wang J, et al. (2011). *AMBER 12*; University of California, San Francisco.
47. Hou T, Wang J, Li Y, Wang W (2011) Assessing the performance of the MM/PBSA and MM/GBSA methods: I. The accuracy of binding free energy calculations based on molecular dynamics simulations. *J Chem Inf Model* 51: 69.
48. Kollman PA, Massova I, Reyes C, Kuhn B, Huo S, et al. (2000) Calculating structures and free energies of complex molecules: combining molecular mechanics and continuum models. *Acc Chem Res* 33: 889-897.
49. Wang W, Donini O, Reyes CM, Kollman PA (2001) Biomolecular simulations: recent developments in force fields, simulations of enzyme catalysis, protein-ligand, protein-protein, and protein-nucleic acid noncovalent interactions. *Annu Rev Biophys Biomol Struct* 30: 211-243.
50. Wang J, Hou T, Xu X (2006) Recent advances in free energy calculations with a combination of molecular mechanics and continuum models. *Curr Comput Aided Drug Des* 2: 287-306.
51. Massova I, Kollman PA (2000) Combined molecular mechanical and continuum solvent approach (MM-PBSA/GBSA) to predict ligand binding. *SAR QSAR Environ Res* 18: 113-135.
52. The UniProt Consortium (2017) UniProt: the universal protein knowledgebase. *Nucleic Acids Res* 45: D158-D169.
53. Rose PW, Prlić A, Altunkaya A, Bi C, Bradley AR, et al. (2017) The RCSB protein data bank: integrative view of protein, gene and 3D structural information. *Nucleic Acids Res* 45: D271-D281
54. Berman HM, Westbrook J, Feng Z, Gilliland G, Bhat TN, et al. (2000) The protein data bank. *Nucleic acids res* 28: 235-242.
55. Yang J, Yan R, Roy A, Xu D, Poisson J, et al. (2015) The I-TASSER Suite: protein structure and function prediction. *Nature methods* 12: 7-8.
56. Roy A, Kucukural A, Zhang Y (2010) I-TASSER: a unified platform for automated protein structure and function prediction. *Nat prot* 5: 725-738.
57. Zhang Y (2008) I-TASSER server for protein 3D structure prediction. *BMC bioinformatics* 9: 40.
58. Zhang Y, Skolnick J (2005) TM-align: a protein structure alignment algorithm based on the TM-score. *Nucleic acids res* 33: 2302-2309.
59. Lovell SC, Davis IW, Arendall WB, De Bakker PI, Word JM, et al. (2003) Structure validation by Ca geometry: ϕ , ψ and C β deviation. *Protein Struct Funct Bio* 50: 437-450.
60. Bowie JU, Luthy R, Eisenberg D (1991) A method to identify protein sequences that fold into a known three-dimensional structure. *Science* 253: 164-170.
61. Luthy R, Bowie JU, Eisenberg D (1992) Assessment of protein models with three-dimensional profiles. *Nature* 356: 83.
62. Geourjon C, Deleage G (1995) SOPMA: significant improvements in protein secondary structure prediction by consensus prediction from multiple alignments. *Comput Appl Biosci*: CABIOS 11: 681-684.
63. Kim S, Thiessen PA, Bolton EE, Chen J, Fu G, et al. (2016) PubChem substance and compound databases. *Nucleic acids res* 44: D1202-1213.
64. O'Boyle NM, Banck M, James CA, Morley C, Vandermeersch T, et al. (2011) Open Babel: An open chemical toolbox. *J Cheminformatics* 3: 33.
65. Hornak V, Abel R, Okur A, Strockbine B, Roitberg A, et al. (2006) Comparison of multiple Amber force fields and development of improved protein backbone parameters. *Protein Struct Funct Bio* 65: 712-725.
66. Wang J, Wolf RM, Caldwell JW, Kollman PA, Case DA (2004) Development and testing of a general amber force field. *J Comput Chem* 25: 1157-1174.
67. Jakalian A, Bush BL, Jack DB, Bayly CI (2000) Fast, efficient generation of high-quality atomic charges. AM1-BCC model: I. Method. *J Comput Chem* 21: 132-146.
68. Jakalian A, Jack DB, Bayly CI (2002) Fast, efficient generation of high-quality atomic charges. AM1-BCC model: II. Parameterization and validation. *J Comput Chem* 23:1623-1641.
69. Jorgensen WL, Chandrasekhar J, Madura JD, Impey RW, Klein ML (1983) Comparison of simple potential functions for simulating liquid water. *J Chem Phys* 79: 926-935.
70. Darden T, York D, Pedersen L (1993) Particle mesh Ewald: An $N \cdot \log(N)$ method for Ewald sums in large systems. *J Chem Phys* 98: 10089-10092.
71. Salomon-Ferrer R, Götz AW, Poole D, Le Grand S, Walker RC (2013). Routine microsecond molecular dynamics simulations with AMBER on GPUs. 2. Explicit solvent particle mesh Ewald. *J Chem Theory Comput* 9: 3878-3888.
72. Berendsen HJ, Postma JV, Van Gunsteren WF, DiNola ARHJ, Haak JR (1984) Molecular dynamics with coupling to an external bath. *J Chem Phys* 81:3684-3690.
73. Ryckaert JP, Ciccotti G, Berendsen HJ (1977) Numerical integration of the cartesian equations of motion of a system with constraints: molecular dynamics of n-alkanes. *J Comput Phys* 23:327-341.

74. Roe DR, Cheatham III TE (2013) PTRAJ and CPPTRAJ: Software for processing and analysis of molecular dynamics trajectory data. *J Chem Theory Comput* 9: 3084-3095.
75. Pettersen EF, Goddard TD, Huang CC, Couch GS, Greenblatt DM, et al. (2004) UCSF Chimera—a visualization system for exploratory research and analysis. *J Chem Theory Comput* 25: 1605-1612.
76. Humphrey W, Dalke A, Schulten K (1996) VMD: Visual molecular dynamics. *J Mol Graph* 14: 33-38.
77. Onufriev A, Bashford D, Case DA (2004) Exploring protein native states and large-scale conformational changes with a modified generalized born model. *Protein Struct Funct Bio* 55: 383-394.
78. Gohlke H, Kiel C, Case DA (2003) Insights into protein-protein binding by binding free energy calculation and free energy decomposition for the Ras-Raf and Ras-RalGDS complexes. *J mol biol* 330: 891-913.
79. Singh RP, Singh A, Kushwaha GS, Singh AK, Kaur P, et al. (2015) Mode of binding of the antithyroid drug propylthiouracil to mammalian haem peroxidases. *Acta Crystallogr. F* 71: 304-310.
80. Singh AK, Singh N, Sinha M, Bhushan A, Kaur P, et al. (2009) Binding modes of aromatic ligands to mammalian heme peroxidases with associated functional implications: Crystal structures of lactoperoxidase complexes with acetylsalicylic acid, salicylhydroxamic acid, and benzyhydroxamic acid. *J Biol Chem* 284: 20311-20318.
81. Arnhold J, Flemmig J (2010). Human myeloperoxidase in innate and acquired immunity. *Arch Biochem Biophys* 500: 92-106.
82. Singh AK, Singh N, Tiwari A, Sinha M, Kushwaha GS, et al. (2010) First structural evidence for the mode of diffusion of aromatic ligands and ligand-induced closure of the hydrophobic channel in heme peroxidases. *J Biol Inorg Chem* 15: 1099-1107.
83. Nakamura H, Noh JY, Itoh K, Fukata S, Miyauchi A, et al. (2007) Comparison of Methimazole and Propylthiouracil in Patients with Hyperthyroidism Caused by Graves' Disease. *J Clin Endocrinol Metab* 92: 2157-2162.
84. Urquiza NM, Naso LG, Martínez Medina JJ, Moyano MA, Lezama L, et al. (2016) Pharmacological activities of a propylthiouracil compound structurally modified by coordination with copper(II). *J Coord Chem* 69: 1293-1312.
85. Tappa VK, John M, Laxikanth C, Numbury SB (2016). Computational studies for inhibitory action of 2-mercapto-1-methylimidazole tautomers on steel using of density functional theory method (DFT). *J Chem Theory Comput* 4: 1-6.
86. Gupta MK, Misra K (2013) Modeling and simulation analysis of propylthiouracil (PTU), an anti-thyroid drug on thyroid peroxidase (TPO), thyroid stimulating hormone receptor (TSHR), and sodium iodide (NIS) symporter based on systems biology approach. *Netw Model Anal Health Inform Bioinform* 2: 45-57.
87. Duan Q, Wang T, Zhang N, Perera V, Liang P, et al. (2016) Propylthiouracil, perchlorate, and thyroid-stimulating hormone modulate high concentrations of iodide instigated mitochondrial superoxide production in the thyroids of metallothionein I/II knockout mice. *J Clin Endocrinol Metab* 31: 174.
88. Bhabak KP, Mughesh G (2010) Inhibition of peroxidase-catalyzed protein tyrosine nitration by antithyroid drugs and their analogues. *Inorganica Chimica Acta* 363: 2812-2818.
89. Manna D, Roy G, Mughesh G (2013) Anti-thyroid drugs and their analogues: Synthesis, structure, and mechanism of action. *Acc Chem Res* 46: 2706-2715.